International Journal of Mathematical Archive-8(2), 2017, 189-203
Available online through www.ijma.info ISSN 2229 – 5046

MHD FREE CONVECTIVE HEAT AND MASS TRANSFER FLOW PAST A LINEARLY ACCELERATED PLATE WITH VARIABLE TEMPERATURE AND MASS DIFFUSION

[1*]G. MUNI SARALA, [1]S. V. K. VARMA AND [2]B. RAMANA

[1]Department of Mathematics, S. V. University, Tirupati, India.

[2]Department of S&H, QIS College of Engg & Tech., Ongole, India.

(Received On: 17-01-17; Revised & Accepted On: 27-02-17)

ABSTRACT

An investigation of MHD free convective heat and mass transfer flow of a viscous, incompressible and radiating fluid past a linearly accelerated transfinite vertical porous plate in the presence of heat absorption, first order chemical reaction is carried out. The governing partial differential equations are converted into non-dimensional form and evolved analytically by applying Laplace transform technique in two cases namely (i) exponentially variable surface temperature (EVST) and linearly variable surface concentration (LVSC) and (ii) linearly variable surface temperature (LVST) and exponentially variable surface concentration (EVSC). Further the expressions for skin friction, Nusselt number and Sherwood number are also derived. The effects of system parameters entering into the present problem on flow quantities such as fluid velocity, fluid temperature and species concentration are depicted graphically. Numerical values of skin friction, Nusselt number and Sherwood number at the plate are presented in tabular form for various values of relevant flow parameters.

Key Words: *Chemical reaction, mass transfer, thermal radiation, porous medium, heat absorption, vertical plate.*

1. INTRODUCTION

Free convection induced by the simultaneous action of buoyancy forces from heat and mass transfer is of significant interest in many industrial applications such as drying processes, solidification of binary alloy, geophysics and oceanography. Especially, the effect of magnetic field on free convective flows is important in electrolytes, ionized gases and liquid metals. Hydromagnetic free convective flows with heat and mass transfer through porous medium have very important applications. Particularly, in the fields of chemical engineering for purification and filtration processes, in petroleum technology for the flow of oil through porous rocks and in the case of drug permeation through human skin.

The radiative heat and mass transfer play an important role for the design of reliable equipment in manufacturing industries. The effect of heat generation or absorption in moving fluids is very important in various physical problems such as fluids undergoing exothermic or endothermic chemical reactions. In most of the chemical engineering processes, chemical reactions take place between a foreign mass and the working fluid which moves due to the stretching of a surface. This sue is involved in various industrial usages such as manufacturing of glassware or ceramics, food processing and polymer production. The order of the chemical reaction depends on several factors. If the rate of reaction is directly proportional to the species concentration, then the chemical reaction is of first order. The study of heat and mass transfer with thermal radiation, chemical reaction has considerable role in chemical and hydrometallurgical industries.

Asogwa et al. [1] investigated the consequences of radiation and chemical reaction on exponentially accelerated infinite vertical plate with exponentially variable temperature and linearly variable concentration. Chamkha [2] discussed heat and mass transfer by laminar flow of a Newtonian fluid on a vertical permeable surface in the presence of magnetic field, first order chemical reaction and heat generation/absorption. The effect of free convection currents on the oscillatory flow through a porous medium bounded by vertical plane surface of constant temperature was given by Hiremath and Patil [3]. Muthucumaraswamy *et al.* [4] analyzed hydromagnetic flow of a viscous incompressible fluid past an impulsively started infinite vertical isothermal plate with variable temperature and concentration. The effects of heat and mass transfer on free convective flow past a vertical plate embedded in a porous medium with uniform permeability in the presence of magnetic field, heat source and chemical reaction have been studied by Pattnaik *et al.* [5].

Corresponding Author: [1]G. Muni Sarala*

Rajesh and Varma [6] performed an analysis on unsteady free convective flow of a viscous fluid past a vertical plate through porous medium with variable temperature or variable mass diffusion in the presence of thermal radiation, magnetic field. Radiation effects on MHD flow of unsteady viscous incompressible fluid past a vertical plate with variable heat and mass transfer were studied by Rajput and Kumar [7]. MHD effects on impulsively started vertical infinite plate with linearly variable temperature in the presence of transverse magnetic field were studied by Soundalgekar *et al.* [8]. Characteristics of heat and mass transfer with linearly variable temperature and exponentially variable species concentration in the presence of heat generation or absorption were presented by Uwanta and Sarki [9].

The purpose of the present flow problem is to analyze the effects of thermal radiation and heat absorption on the flow past a linearly accelerated transfinite vertical plate with chemical reaction. The dimensionless governing equations are solved by using the Laplace transform technique. The solutions are expressed in terms of exponential and complementary error functions.

2. MATHEMATICAL FORMULATION

Consider unsteady two-dimensional MHD free convective heat and mass transfer flow of a viscous, incompressible, electrically conducting, heat absorbing, radiating and chemically reactive fluid past a linearly accelerated transfinite vertical porous plate with variable temperature and mass diffusion. According to the cartesian coordinate system (x^*, y^*), the x^*-axis is chosen along the plate in the vertically upward direction and the y^*-axis is taken normal to the plate into the fluid by assuming an arbitrary point on this plate as the origin. Initially, at time $t^* \le 0$, the plate and the fluid are at the same temperature T_∞^* and concentration level C_∞^* in a stationary condition for all the points. At time $t^* > 0$, the plate is linearly accelerated with a velocity $u^* = u_0 t^*$ in its own plane along the x^*-axis against the gravitational field. As the plate is transfinite extent in the x^* direction, all the physical quantities are independent of x^* and are functions of y^* and time t^* only. Then under usual Boussinesq estimation, the unsteady flow of a radiating fluid is governed by the following system of equations.

$$\frac{\partial u^*}{\partial t^*} = \nu \frac{\partial^2 u^*}{\partial y^{*2}} + g\beta(T^* - T_\infty^*) + g\beta^*(C^* - C_\infty^*) - \frac{\sigma B_0^2}{\rho} u^* - \nu \frac{u^*}{K^*} \tag{1}$$

$$\rho C_p \frac{\partial T^*}{\partial t^*} = \kappa \frac{\partial^2 T^*}{\partial y^{*2}} - \frac{\partial q_r^*}{\partial y^*} - Q_0(T^* - T_\infty^*) \tag{2}$$

$$\frac{\partial C^*}{\partial t^*} = D \frac{\partial^2 C^*}{\partial y^{*2}} - K_r^*(C^* - C_\infty^*) \tag{3}$$

and the initial and boundary conditions for this flow are

Case (i):

$$\left.\begin{aligned} & t^* \le 0 : u^* = 0, T^* = T_\infty^*, C^* = C_\infty^* \quad \text{for all } y^* \ge 0 \\ & t^* > 0 : \begin{cases} u^* = u_0 t^*, T^* = T_\infty^* + (T_w^* - T_\infty^*) e^{a^* t^*}, C^* = C_\infty^* + (C_w^* - C_\infty^*) A t^* & \text{at } y^* = 0 \\ u^* \to 0, T^* \to T_\infty^*, C^* \to C_\infty^* & \text{as } y^* \to \infty \end{cases} \end{aligned}\right\} \tag{4a}$$

Case (ii):

$$\left.\begin{aligned} & t^* \le 0 : u^* = 0, T^* = T_\infty^*, C^* = C_\infty^* \quad \text{for all } y^* \ge 0 \\ & t^* > 0 : \begin{cases} u^* = u_0 t^*, T^* = T_\infty^* + (T_w^* - T_\infty^*) A t^*, C^* = C_\infty^* + (C_w^* - C_\infty^*) e^{a^* t^*} & \text{at } y^* = 0 \\ u^* \to 0, T^* \to T_\infty^*, C^* \to C_\infty^* & \text{as } y^* \to \infty \end{cases} \end{aligned}\right\} \tag{4b}$$

where $A = \left(\frac{u_0^2}{\nu}\right)^{1/3}$, A is a constant

By making use of the Rosseland estimation, the term of radiative heat flux q_r^* for an optically thin fluid is given by

$$q_r^* = -\frac{4\sigma^*}{3k^*} \frac{\partial T^{*4}}{\partial y^*} \tag{5}$$

where σ^* is the Stefan-Boltzmann constant and k^* is the mean absorption coefficient. Assuming that the temperature differences between free stream and the fluid in the boundary layer are sufficiently small then the term T^{*4} can be expressed as a linear function of temperature T^*. This is obtained by expanding T^{*4} about free stream T_∞^* in a Taylor's series as follows:

$$T^{*4} = T_\infty^{*4} + 4T_\infty^{*3}(T^* - T_\infty^*) + 6T_\infty^{*2}(T^* - T_\infty^*)^2 + \cdots \tag{6}$$

after neglecting the higher order terms, we get

$$T^{*4} \cong 4T_\infty^{*3}T^* - 3T_\infty^{*4} \tag{7}$$

Differentiating Equation (5) with respect to y^* and using Equation (7), we get

$$\frac{\partial q_r^*}{\partial y^*} = -\frac{16\sigma^* T_\infty^{*3}}{3k^*}\frac{\partial^2 T^*}{\partial y^{*2}} \tag{8}$$

On introducing the non-dimensional succeeding measures

$$\left.\begin{aligned} &u = \frac{u^*}{(\nu u_0)^{1/3}},\ t = t^*\left(\frac{u_0^2}{\nu}\right)^{1/3},\ y = y^*\left(\frac{u_0}{\nu^2}\right)^{1/3},\ a = a^*\left(\frac{\nu}{u_0^2}\right)^{1/3},\ \theta = \frac{T^* - T_\infty^*}{T_w^* - T_\infty^*},\\ &C = \frac{C^* - C_\infty^*}{C_w^* - C_\infty^*}, G_r = \frac{g\beta(T_w^* - T_\infty^*)}{u_0}, G_m = \frac{g\beta^*(C_w^* - C_\infty^*)}{u_0},\ \Pr = \frac{\rho\nu C_p}{\kappa}, Sc = \frac{\nu}{D},\\ &M = \frac{\sigma B_0^2 \nu^{1/3}}{\rho u_0^{2/3}},\ \frac{1}{K} = \frac{\nu^{4/3}}{K^* u_0^{2/3}},\ \gamma = \frac{\nu^{1/3}K_r^*}{u_0^{2/3}},\ R = \frac{16\sigma^* T_\infty^{*3}}{3\kappa k^*},\ Q = \frac{Q_0 \nu^{1/3}}{\rho C_p u_0^{2/3}}, \end{aligned}\right\} \tag{9}$$

By using Equations (8) and (9), the Equations (1) - (3) are reduced to the following non-dimensional forms

$$\frac{\partial u}{\partial t} = \frac{\partial^2 u}{\partial y^2} + G_r\theta + G_m C - \left(M + \frac{1}{K}\right)u \tag{10}$$

$$\frac{\partial \theta}{\partial t} = \left(\frac{1+R}{\Pr}\right)\frac{\partial^2 \theta}{\partial y^2} - Q\theta \tag{11}$$

$$\frac{\partial C}{\partial t} = \frac{1}{Sc}\frac{\partial^2 C}{\partial y^2} - \gamma C \tag{12}$$

In non-dimensional form, the initial and boundary conditions reduced to as follows

Case (i):

$$\left.\begin{aligned} &t \le 0 : u = 0, \theta = 0, C = 0 \ \text{ for all } y \ge 0\\ &t > 0 : \begin{cases} u = t,\ \theta = e^{at},\ C = t & \text{at } y = 0\\ u \to 0,\ \theta \to 0,\ C \to 0 & \text{as } y \to \infty \end{cases} \end{aligned}\right\} \tag{13a}$$

Case (ii):

$$\left.\begin{aligned} &t \le 0 : u = 0, \theta = 0, C = 0 \ \text{ for all } y \ge 0\\ &t > 0 : \begin{cases} u = t,\ \theta = t,\ C = e^{at} & \text{at } y = 0\\ u \to 0,\ \theta \to 0,\ C \to 0 & \text{as } y \to \infty \end{cases} \end{aligned}\right\} \tag{13b}$$

3. SOLUTION OF THE PROBLEM

The dimensionless governing equations (10)-(12) subject to the initial and boundary conditions (13) are solved by the usual Laplace transform technique without any restriction and the solutions for velocity, temperature and concentration fields are as follows:

Case (i):

$$u(y,t)=a_3I_1+a_2(I_3-I_4-I_6+I_7)+a_4(I_5-I_2+I_9-I_{10})-a_1I_8 \tag{14}$$

$$\theta(y,t)=I_6 \tag{15}$$

$$C(y,t)=I_8 \tag{16}$$

SKIN FRICTION:

In non-dimensional form, the skin friction at the plate is given by

$$\tau=-\left(\frac{\partial u}{\partial y}\right)_{y=0} \tag{17}$$

From Equations (14) and (17), we get

$$\begin{aligned}\tau=a_3&\left[\sqrt{\frac{t}{\pi}}\exp(-Nt)+\left(t\sqrt{N}+\frac{1}{2\sqrt{N}}\right)erf\left(\sqrt{Nt}\right)\right]\\&+a_2\exp(at)\left[\frac{1}{\sqrt{\pi t}}\exp(-(N+a)t)+\sqrt{N+a}\;erf\left(\sqrt{(N+a)t}\right)\right]\\&-a_2\exp(-bt)\left[\frac{1}{\sqrt{\pi t}}\exp(-(N-b)t)+\sqrt{N-b}\;erf\left(\sqrt{(N-b)t}\right)\right]\\&-a_2\exp(at)\left[\sqrt{\frac{\lambda}{\pi t}}\exp(-(Q+a)t)+\sqrt{(Q+a)\lambda}\;erf\left(\sqrt{(Q+a)t}\right)\right]\\&+a_2\exp(-bt)\left[\sqrt{\frac{\lambda}{\pi t}}\exp(-(Q-b)t)+\sqrt{(Q-b)\lambda}\;erf\left(\sqrt{(Q-b)t}\right)\right]\\&-a_4\left[\frac{1}{\sqrt{\pi t}}\exp(-Nt)+\sqrt{N}\;erf\left(\sqrt{Nt}\right)\right]\\&+a_4\exp(-ct)\left[\frac{1}{\sqrt{\pi t}}\exp(-(N-c)t)+\sqrt{N-c}\;erf\left(\sqrt{(N-c)t}\right)\right]\\&+a_4\left[\sqrt{\frac{Sc}{\pi t}}\exp(-\gamma t)+\sqrt{\gamma Sc}\;erf\left(\sqrt{\gamma t}\right)\right]\\&-a_1\left[\sqrt{\frac{tSc}{\pi}}\exp(-\gamma t)+\left(t\sqrt{\gamma Sc}+\frac{\sqrt{Sc}}{2\sqrt{\gamma}}\right)erf\left(\sqrt{\gamma t}\right)\right]\\&-a_4\exp(-ct)\left[\sqrt{\frac{Sc}{\pi t}}\exp(-(\gamma-c)t)+\sqrt{(\gamma-c)Sc}\;erf\left(\sqrt{(\gamma-c)t}\right)\right]\end{aligned} \tag{18}$$

NUSSELT NUMBER:

In non-dimensional form, rate of change of heat transfer from temperature field is determined and it is in the form of Nusselt number as

$$Nu=-\left(\frac{\partial\theta}{\partial y}\right)_{y=0} \tag{19}$$

From Equations (15) and (19), we obtain the Nusselt number as

$$Nu=\sqrt{\frac{\lambda}{\pi t}}\exp(-Qt)+\sqrt{(Q+a)\lambda}\exp(at)erf\left(\sqrt{(Q+a)t}\right) \tag{20}$$

SHERWOOD NUMBER:

In non-dimensional form, rate of change of mass transfer from concentration field is determined and it is in the form of Sherwood number as

$$Sh = -\left(\frac{\partial C}{\partial y}\right)_{y=0} \tag{21}$$

From Equations (16) and (21), we get

$$Sh = \sqrt{\frac{tSc}{\pi}}\exp(-\gamma t) + \left(t\sqrt{\gamma Sc} + \frac{\sqrt{Sc}}{2\sqrt{\gamma}}\right) erf\left(\sqrt{\gamma t}\right) \tag{22}$$

Case (ii):

$$u(y,t) = a_7 I_1 + a_8(I_4 - I_2 - I_7 + I_{12}) + a_6(I_3 - I_5 + I_{10} - I_{13}) - a_5 I_{11} \tag{23}$$

$$\theta(y,t) = I_{11} \tag{24}$$

$$C(y,t) = I_{13} \tag{25}$$

SKIN FRICTION:

Using Equations (17) and (23), we obtain the skin friction as

$$\begin{aligned}
\tau = a_7 &\left[\sqrt{\frac{t}{\pi}}\exp(-Nt) + \left(t\sqrt{N} + \frac{1}{2\sqrt{N}}\right) erf\left(\sqrt{Nt}\right)\right] \\
&- a_8\left[\frac{1}{\sqrt{\pi t}}\exp(-Nt) + \sqrt{N}\, erf\left(\sqrt{Nt}\right)\right] \\
&+ a_8\exp(-bt)\left[\frac{1}{\sqrt{\pi t}}\exp(-(N-b)t) + \sqrt{N-b}\, erf\left(\sqrt{(N-b)t}\right)\right] \\
&+ a_8\left[\sqrt{\frac{\lambda}{\pi t}}\exp(-Qt) + \sqrt{\lambda Q} erf\left(\sqrt{Qt}\right)\right] \\
&- a_5\left[\sqrt{\frac{\lambda t}{\pi}}\exp(-Qt) + \left(t\sqrt{\lambda Q} + \frac{1}{2}\sqrt{\frac{\lambda}{Q}}\right) erf\left(\sqrt{Qt}\right)\right] \\
&- a_8\exp(-bt)\left[\sqrt{\frac{\lambda}{\pi t}}\exp(-(Q-b)t) + \sqrt{(Q-b)\lambda}\, erf\left(\sqrt{(Q-b)t}\right)\right] \\
&+ a_6\exp(at)\left[\frac{1}{\sqrt{\pi t}}\exp(-(N+a)t) + \sqrt{N+a}\, erf\left(\sqrt{(N+a)t}\right)\right] \\
&- a_6\exp(-ct)\left[\frac{1}{\sqrt{\pi t}}\exp(-(N-c)t) + \sqrt{N-c}\, erf\left(\sqrt{(N-c)t}\right)\right] \\
&- a_6\exp(at)\left[\sqrt{\frac{Sc}{\pi t}}\exp(-(\gamma+a)t) + \sqrt{(\gamma+a)Sc}\, erf\left(\sqrt{(\gamma+a)t}\right)\right] \\
&+ a_6\exp(-ct)\left[\sqrt{\frac{Sc}{\pi t}}\exp(-(\gamma-c)t) + \sqrt{(\gamma-c)Sc}\, erf\left(\sqrt{(\gamma-c)t}\right)\right]
\end{aligned} \tag{26}$$

NUSSELT NUMBER:

Using Equations (19) and (24), we obtain the Nusselt number as

$$Nu = \sqrt{\frac{\lambda t}{\pi}}\exp(-Qt) + \left(t\sqrt{\lambda Q} + \frac{1}{2}\sqrt{\frac{\lambda}{Q}}\right) erf\left(\sqrt{Qt}\right) \tag{27}$$

SHERWOOD NUMBER:

Using Equations (21) and (25), we obtain the Sherwood number as

$$Sh = \sqrt{\frac{Sc}{\pi t}}\exp(-\gamma t) + \sqrt{(\gamma + a)\,Sc}\exp(at)\, erf\left(\sqrt{(\gamma + a)t}\right) \tag{28}$$

where

$$N = M + \frac{1}{K},\ \lambda = \frac{\Pr}{1+R},\ b = \frac{\lambda Q - N}{\lambda - 1},\ c = \frac{\gamma Sc - N}{Sc - 1},$$

$$a_1 = \frac{G_m}{c(Sc-1)},\ a_2 = \frac{G_r}{(\lambda-1)(a+b)},\ a_3 = 1 + a_1,\ a_4 = \frac{a_1}{c},$$

$$a_5 = \frac{G_r}{b(\lambda-1)},\ a_6 = \frac{G_m}{(Sc-1)(a+c)},\ a_7 = 1 + a_5,\ a_8 = \frac{a_5}{b},$$

$$I_1 = \left(\frac{t}{2} + \frac{y}{4\sqrt{N}}\right)\exp\left(y\sqrt{N}\right) erfc\left(\frac{y}{2\sqrt{t}} + \sqrt{Nt}\right) + \left(\frac{t}{2} - \frac{y}{4\sqrt{N}}\right)\exp\left(-y\sqrt{N}\right) erfc\left(\frac{y}{2\sqrt{t}} - \sqrt{Nt}\right)$$

$$I_2 = \frac{1}{2}\left[\exp\left(y\sqrt{N}\right) erfc\left(\frac{y}{2\sqrt{t}} + \sqrt{Nt}\right) + \exp\left(-y\sqrt{N}\right) erfc\left(\frac{y}{2\sqrt{t}} - \sqrt{Nt}\right)\right]$$

$$I_3 = \frac{\exp(at)}{2}\left[\exp\left(y\sqrt{N+a}\right) erfc\left(\frac{y}{2\sqrt{t}} + \sqrt{(N+a)t}\right) + \exp\left(-y\sqrt{N+a}\right) erfc\left(\frac{y}{2\sqrt{t}} - \sqrt{(N+a)t}\right)\right]$$

$$I_4 = \frac{\exp(-bt)}{2}\left[\exp\left(y\sqrt{N-b}\right) erfc\left(\frac{y}{2\sqrt{t}} + \sqrt{(N-b)t}\right) + \exp\left(-y\sqrt{N-b}\right) erfc\left(\frac{y}{2\sqrt{t}} - \sqrt{(N-b)t}\right)\right]$$

$$I_5 = \frac{\exp(-ct)}{2}\left[\exp\left(y\sqrt{N-c}\right) erfc\left(\frac{y}{2\sqrt{t}} + \sqrt{(N-c)t}\right) + \exp\left(-y\sqrt{N-c}\right) erfc\left(\frac{y}{2\sqrt{t}} - \sqrt{(N-c)t}\right)\right]$$

$$I_6 = \frac{\exp(at)}{2}\left[\exp\left(y\sqrt{(Q+a)\lambda}\right) erfc\left(\frac{y\sqrt{\lambda}}{2\sqrt{t}} + \sqrt{(Q+a)t}\right) - \exp\left(-y\sqrt{(Q+a)\lambda}\right) erfc\left(\frac{y\sqrt{\lambda}}{2\sqrt{t}} - \sqrt{(Q+a)t}\right)\right]$$

$$I_7 = \frac{\exp(-bt)}{2}\left[\exp\left(y\sqrt{(Q-b)\lambda}\right) erfc\left(\frac{y\sqrt{\lambda}}{2\sqrt{t}} + \sqrt{(Q-b)t}\right) + \exp\left(-y\sqrt{(Q-b)\lambda}\right) erfc\left(\frac{y\sqrt{\lambda}}{2\sqrt{t}} - \sqrt{(Q-b)t}\right)\right]$$

$$I_8 = \left(\frac{t}{2} + \frac{y\sqrt{Sc}}{4\sqrt{\gamma}}\right)\exp\left(y\sqrt{\gamma Sc}\right) erfc\left(\frac{y\sqrt{Sc}}{2\sqrt{t}} + \sqrt{\gamma t}\right) + \left(\frac{t}{2} - \frac{y\sqrt{Sc}}{4\sqrt{\gamma}}\right)\exp\left(-y\sqrt{\gamma Sc}\right) erfc\left(\frac{y\sqrt{Sc}}{2\sqrt{t}} - \sqrt{\gamma t}\right)$$

$$I_9 = \frac{1}{2}\left[\exp\left(y\sqrt{\gamma Sc}\right) erfc\left(\frac{y\sqrt{Sc}}{2\sqrt{t}} + \sqrt{\gamma t}\right) + \exp\left(-y\sqrt{\gamma Sc}\right) erfc\left(\frac{y\sqrt{Sc}}{2\sqrt{t}} - \sqrt{\gamma t}\right)\right]$$

$$I_{10} = \frac{\exp(-ct)}{2}\left[\exp\left(y\sqrt{(\gamma-c)Sc}\right) erfc\left(\frac{y\sqrt{Sc}}{2\sqrt{t}} + \sqrt{(\gamma-c)t}\right) + \exp\left(-y\sqrt{(\gamma-c)Sc}\right) erfc\left(\frac{y\sqrt{Sc}}{2\sqrt{t}} - \sqrt{(\gamma-c)t}\right)\right]$$

$$I_{11} = \left(\frac{t}{2} + \frac{y}{4}\sqrt{\frac{\lambda}{Q}}\right)\exp\left(y\sqrt{\lambda Q}\right) erfc\left(\frac{y\sqrt{\lambda}}{2\sqrt{t}} + \sqrt{Qt}\right) + \left(\frac{t}{2} - \frac{y}{4}\sqrt{\frac{\lambda}{Q}}\right)\exp\left(-y\sqrt{\lambda Q}\right) erfc\left(\frac{y\sqrt{\lambda}}{2\sqrt{t}} - \sqrt{Qt}\right)$$

$$I_{12} = \frac{1}{2}\left[\exp\left(y\sqrt{\lambda Q}\right) erfc\left(\frac{y\sqrt{\lambda}}{2\sqrt{t}} + \sqrt{Qt}\right) + \exp\left(-y\sqrt{\lambda Q}\right) erfc\left(\frac{y\sqrt{\lambda}}{2\sqrt{t}} - \sqrt{Qt}\right)\right]$$

$$I_{13}=\frac{\exp(at)}{2}\left[\exp\left(y\sqrt{(\gamma+a)Sc}\right)erfc\left(\frac{y\sqrt{Sc}}{2\sqrt{t}}+\sqrt{(\gamma+a)t}\right)+\exp\left(-y\sqrt{(\gamma+a)Sc}\right)erfc\left(\frac{y\sqrt{Sc}}{2\sqrt{t}}-\sqrt{(\gamma+a)t}\right)\right]$$

4. RESULTS AND DISCUSSION

In the previous section, analytical solutions for the velocity u, temperature θ, species concentration C, skin friction τ, Nusselt number Nu and Sherwood number Sh have been obtained by using Laplace transform technique in terms of the system parameters for two cases. Numerical computations of the velocity, temperature, concentration, skin friction, Nusselt number and Sherwood number are computed for different physical parameters like Magnetic field parameter (M), Thermal Grashof number (G_r), Mass Grashof number (G_m), Permeability parameter (K), Radiation parameter (R), Heat source parameter (Q), Chemical reaction rarameter (γ), acceleration paramater (a), time (t) and for fixed values of Prandtl number (Pr), Schmidt number (Sc) in two cases namely, (i) exponentially variable surface temperature and linearly variable surface concentration from figures 1 to 8 and (ii) linearly variable surface temperature and exponentially variable surface concentration from figures 9 to 16 with tables 1 to 3. Here the results are limited to Pr values $\mathrm{Pr}=0.71$ (air), 7.0 (water), and the values of Sc are chosen such that $Sc=0.22$ (hydrogen), 0.30 (helium), 0.60 (water vapour), 0.78 (ammonia).

In order to validate the accuracy of numerical results, the present study is compared with the results of Uwanta and Sarki [9] in Figure 17 in the absence of radiation parameter, magnetic field parameter and permeability parameter for **case (ii)** and the results are found to be in good agreement.

Case (i): Figures 1 to 5 reveal the graphs of velocity profiles under the influence of magnetic field parameter, Grashof number for heat and mass transfer, radiation parameter, heat source parameter, permeability parameter, chemical reaction parameter, Schmidt number, Prandtl number, acceleration parameter and time when the plate is cooled by free convective currents $(G_r>0, G_m>0)$. Figure 1 displays the effect of magnetic field parameter on transient velocity for $\mathrm{Pr}=0.71$. As expected, we observed that an increase in magnetic parameter reduces the velocity. The effects of thermal Grashof number (G_r), mass Grashof number (G_m) and time (t) on the velocity field are plotted in Figure 2. The trend shows that the velocity increases as G_r or G_m or t increases. Figure 3 indicates the effects of radiation parameter and heat source parameter. It is found that an increase in radiation parameter leads to an increase in the velocity in the presence of constant heat source parameter, but reverse effect is noted in respect of heat source parameter. Moreover, the presence of radiation is found to be favourable in enhancing the velocity.

The velocity profiles for different values of chemical reaction parameter and Schmidt number are plotted in Figure 4. It is seen that from this figure an increase in the values of chemical reaction parameter and Schmidt number causes the velocity decreases. Figure 5 describes the effects of permeability parameter and acceleration parameter at $t=2$ on the velocity profiles. From this figure it is seen that the velocity increases with an increase in the permeability parameter and acceleration parameter.

The temperature profiles for various values of radiation parameter, heat source parameter and time are presented in Figure 6. It is found that the temperature increases as radiation parameter or time increases while it decreases with increasing values of heat source parameter. The temperature distribution θ against y for various values of acceleration parameter and Prandtl number is shown in Figure 7. It is evident that the temperature increases with increasing acceleration parameter, but falls owing to an increase in the Prandtl number. Figure 8 describes the effects of chemical reaction parameter, Schmidt number and time on concentration field. It is significant that the concentration increases with increasing time where as it decreases with increasing chemical reaction parameter and Schmidt number. When the plate is heated by free convection currents $(G_r<0, G_m<0)$, exactly the reverse trend is noticed in all these cases from numerical computations. To avoid space consumption figures are not provided.

Numerical evaluations of skin friction coefficient (τ), Nusselt number (Nu) and Sherwood number (Sh) are provided in Tables 1-3. It is mentioned that the comparison of each physical parameter is made with first row in the corresponding table. The behaviour of skin friction coefficient at the plate is shown in Table 1 for various values of physical parameters. In the case of cooling $(G_r>0, G_m>0)$ of the plate, it is noticed that an increase in the magnetic field parameter or heat source parameter or Schmidt number or chemical reaction parameter or Prandtl number or time leads to a rise in the skin friction while an increase in the thermal Grashof number or modified Grashof number or radiation parameter or permeability parameter or acceleration parameter leads to a fall in the skin friction. In case of heating plate exactly opposite trend is noted from numerical evaluations.

Numerical values of the rate of heat transfer in terms of Nusselt number are presented in Table 2 for different values of radiation parameter, heat source parameter, Prandtl number, and time. From this table, the Nusselt number increases with increasing heat source parameter while it decreases with increasing radiation parameter. Also it is depicted with increasing values of Pr and t, the Nusselt number increases.

Finally, Table 3 represents the numerical values of the rate of mass transfer in terms of Sherwood number due to variations in Schmidt number or chemical reaction parameter or time. It is observed that Sherwood number increases on increasing Schmidt number or chemical reaction parameter or time.

Case (ii): When the plate is cooled by free convective currents $(G_r > 0, G_m > 0)$, Figures 9 to 13 demonstrate the velocity profiles u against y for different values of magnetic field parameter, thermal Grashof number, mass Grashof number, radiation parameter, heat source parameter, permeability parameter, chemical reaction parameter, Schmidt number, Prandtl number, acceleration parameter and time. The velocity decreases as the magnetic field parameter increases and is depicted in Figure 9. For various values of thermal buoyancy and mass buoyancy, the velocity distribution is presented in Figure 10. From this figure it is clear that an increase in thermal buoyancy and mass buoyancy leads to increase the fluid velocity.

Figure 11 displays the effects of radiation parameter and heat source parameter on the fluid velocity. It is found that with increasing radiation parameter and decreasing heat source parameter, the velocity increases. Figure 12 is sketched in order to discuss the variations of Schmidt number and chemical reaction parameter for both $\Pr = 0.71$ (air) and $\Pr = 7.0$ (water). From this figure, it is evident the velocity decreases with increasing values of chemical reaction parameter and Schmidt number for both air and water. Also, it is clear that the velocity for air is higher than that of water.

An increase in the acceleration parameter and permeability parameter, the velocity increases and is shown in Figure 13. Also, it is noticed from this figure the velocity is getting enhanced as time progresses. The behaviour of radiation parameter, heat source parameter and time on temperature field is presented in Figure 14. It is noticed that an increase in radiation parameter or time results a significant rise in the temperature while the opposite trend is observed with increasing strength of heat source parameter. Figure 15 illustrates the influence of chemical reaction parameter and acceleration parameter at time $t = 2$ on the concentration field. It is clear that the concentration decreases with increasing chemical reaction parameter whereas the reverse effect is observed in case of acceleration parameter.

Finally, from Figure 16 it is revealed that the concentration decreases with increasing Schmidt number. Likewise, species concentration is enhanced with increasing time. When the plate is heated by free convection currents $(G_r < 0, G_m < 0)$, exactly reverse trend is observed in all these cases from numerical computations. Figures are not extended to avoid space consumption.

The numerical values of skin friction for cooling $(G_r > 0, G_m > 0)$ of the plate are provided in Table 1. The skin friction increases with increasing of M or Q or Sc or Pr or γ or t while it decreases as G_r or G_m or R or K or a increases. The behaviour of rate of heat transfer at the plate Nu under the influence of R, Q, Pr and t are displayed in Table 2. It is depicted from Table 2 that Nu increases on increasing Q or Pr or t whereas it decreases on increasing R. Numerical values of rate of mass transfer at the plate Sh are presented in Table 3 for different values of Sc, γ and t. It is clear form Table 3 that Sh increases as Sc or γ or t increases.

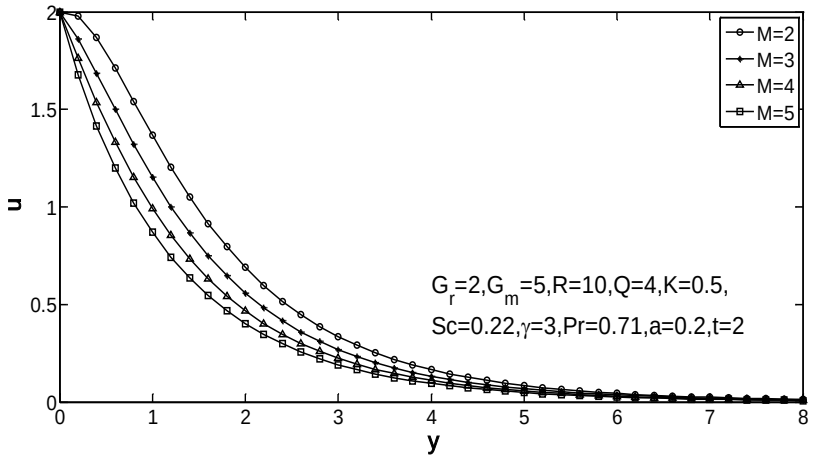

Figure-1: Velocity profiles for different values of M

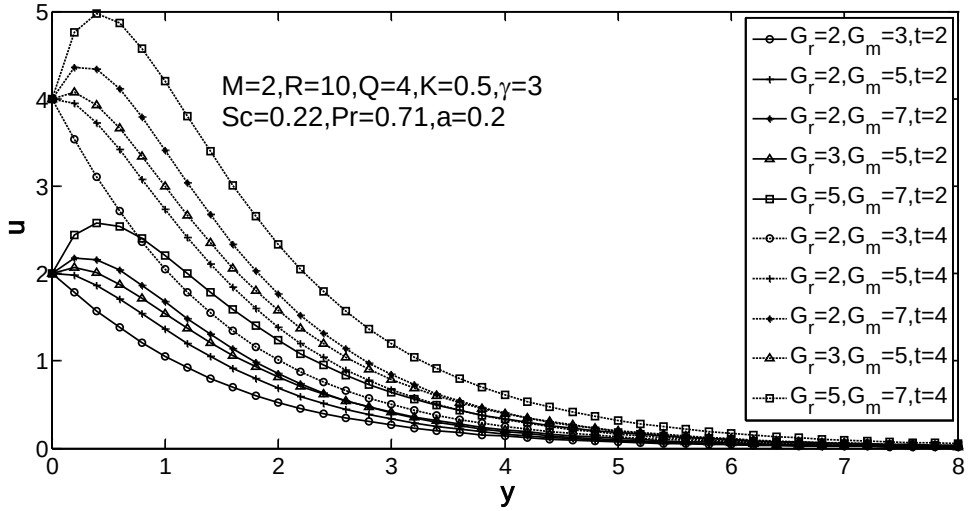

Figure-2: Velocity profiles for different values of G_r, G_m and t

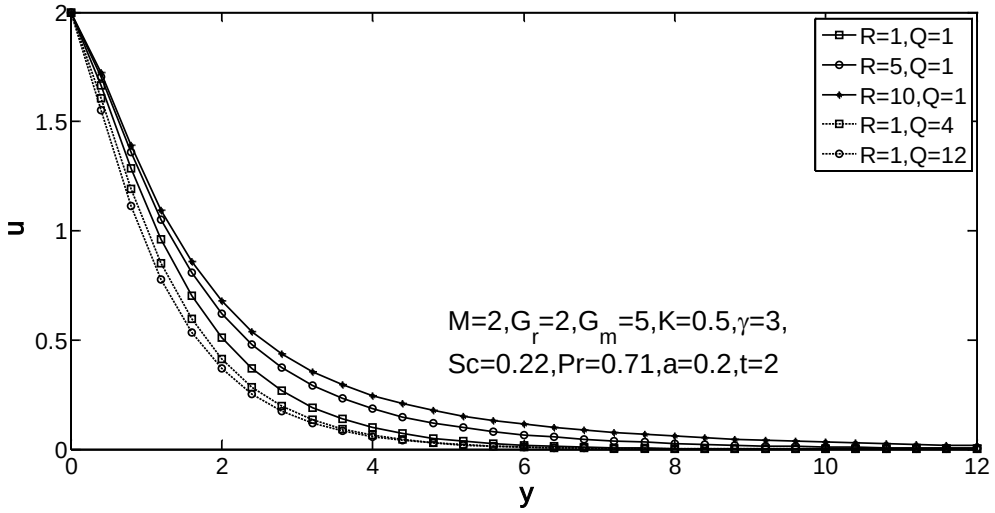

Figure-3: Velocity profiles for different values of R and Q

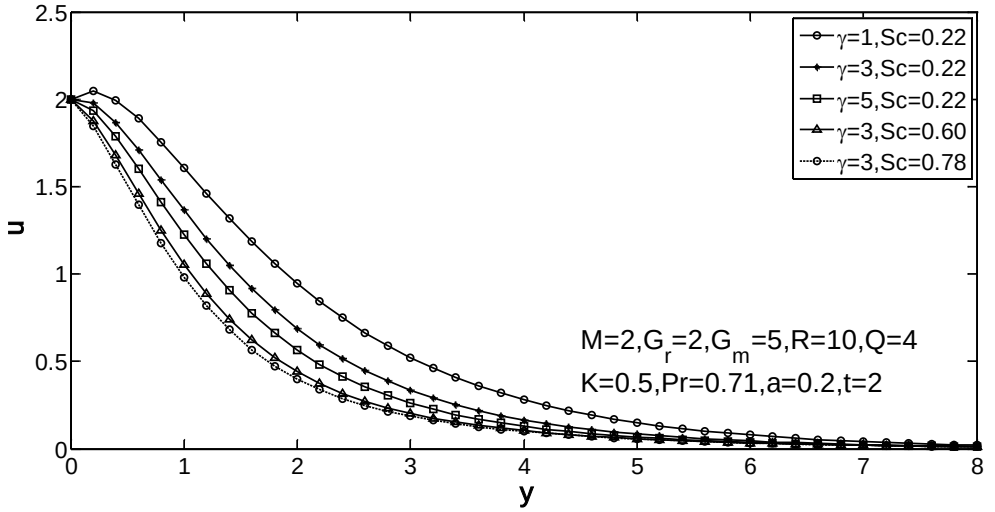

Figure-4: Velocity profiles for different values of γ and Sc

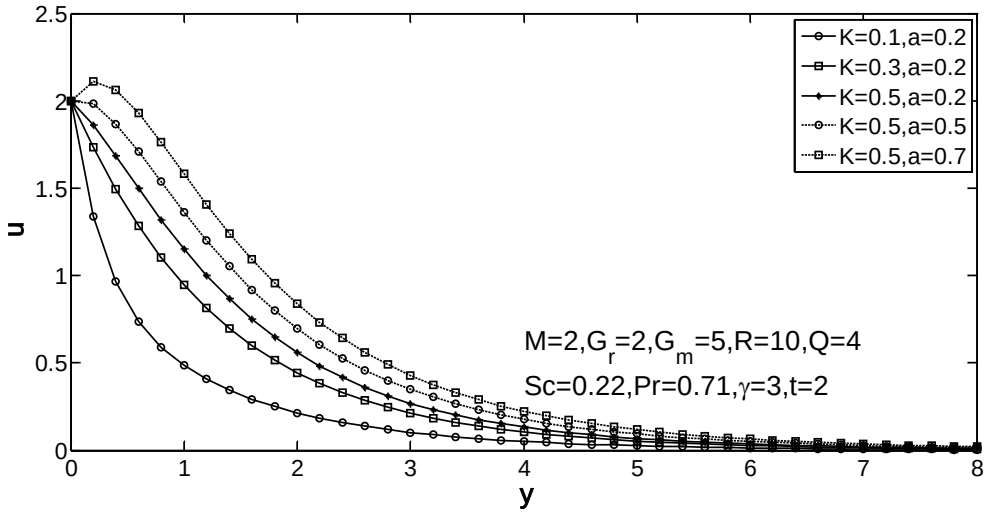

Figure-5: Velocity profiles for different values of K and a

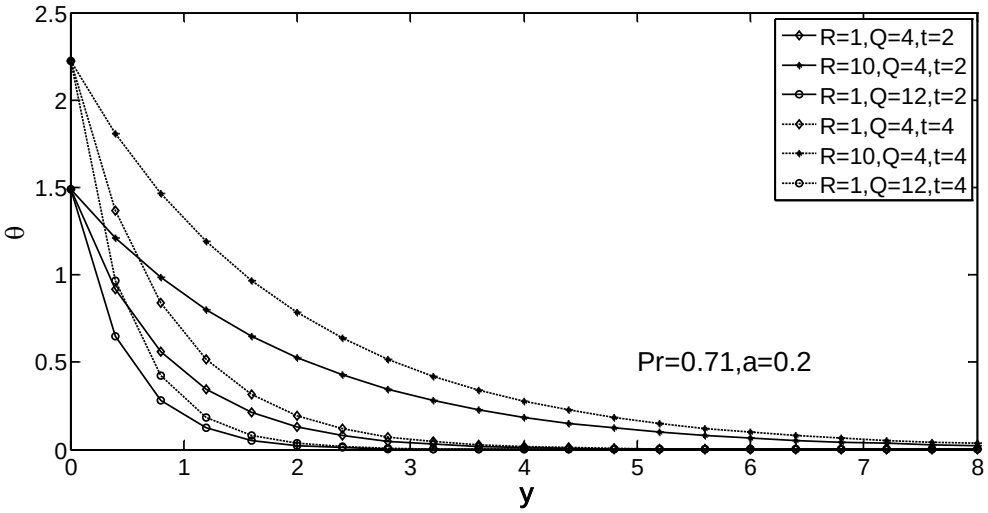

Figure-6: Temperature profiles for different values of R and Q

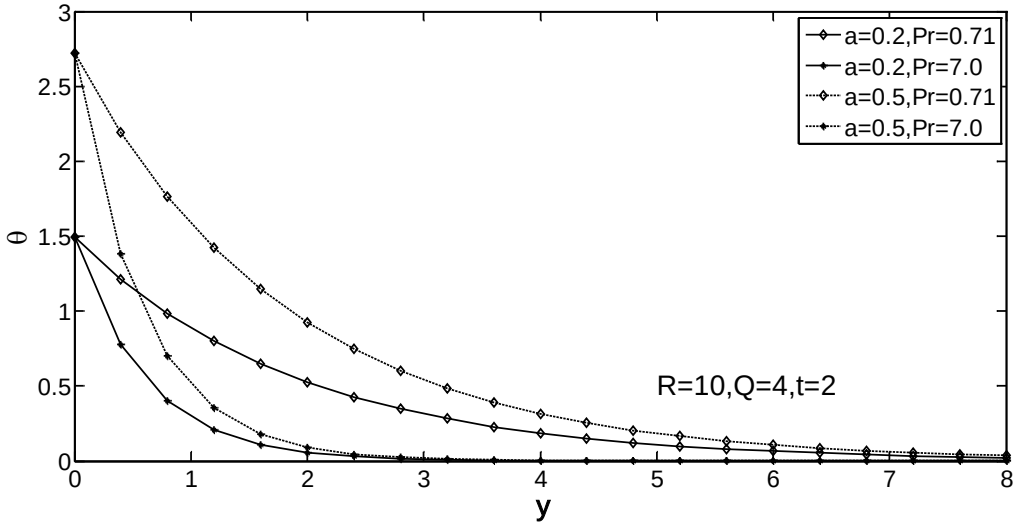

Figure-7: Temperature profiles for different values of a and $\Pr$

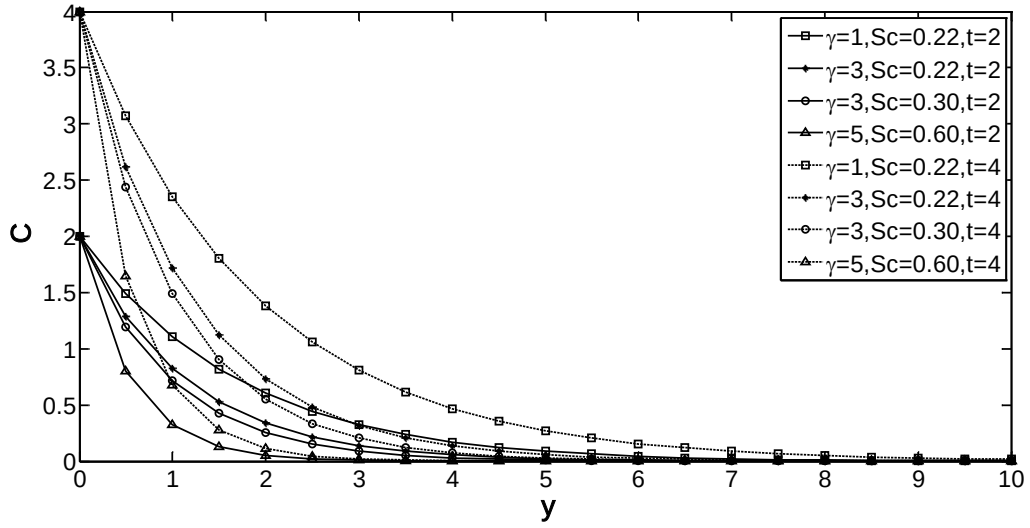

Figure-8: Concentration profiles for different values of γ, Sc and t

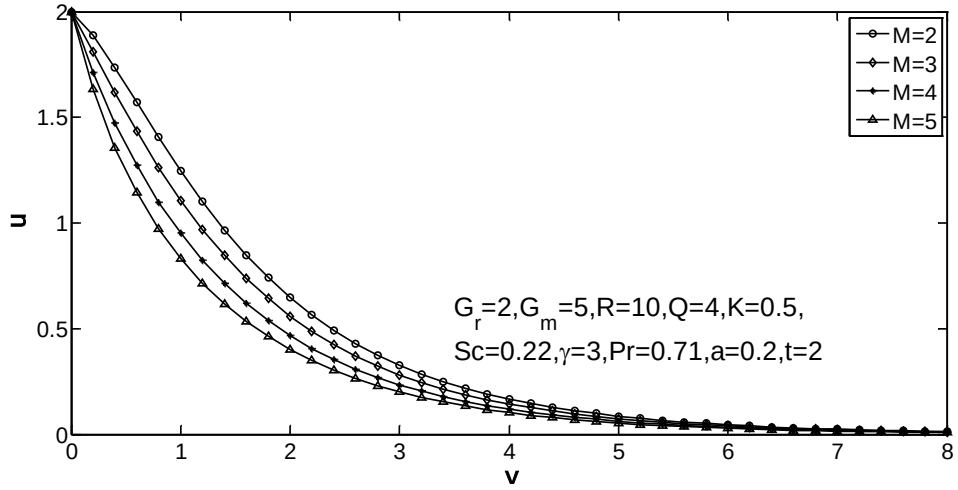

Figure-9: Velocity profiles for different values of M

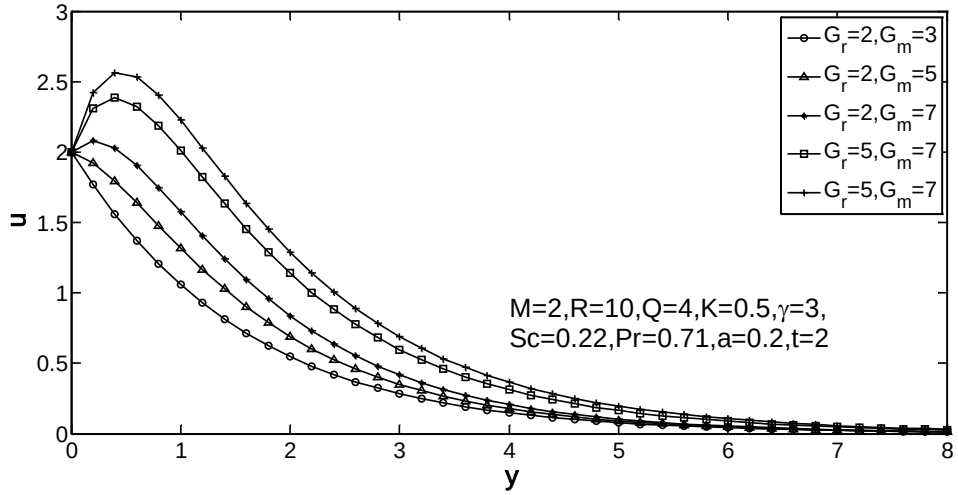

Figure-10: Velocity profiles for different values of G_r and G_m

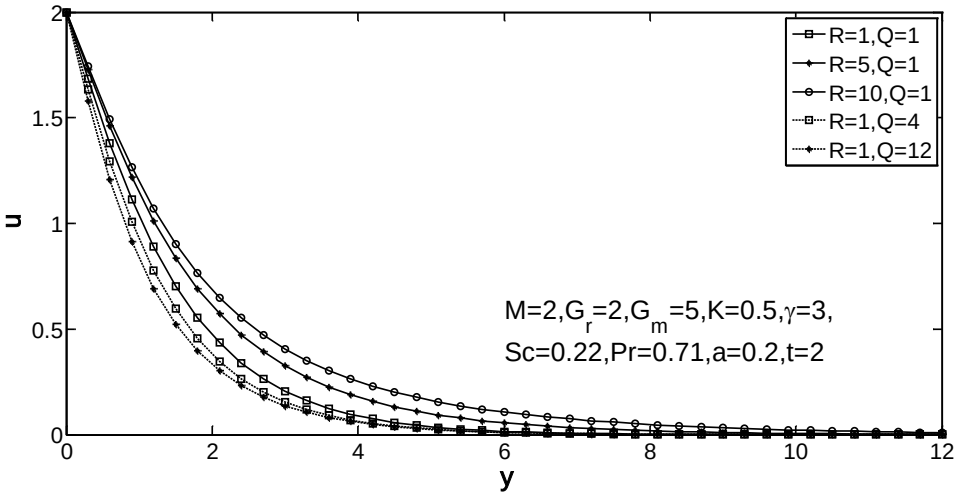

Figure-11: Velocity profiles for different values of R and Q

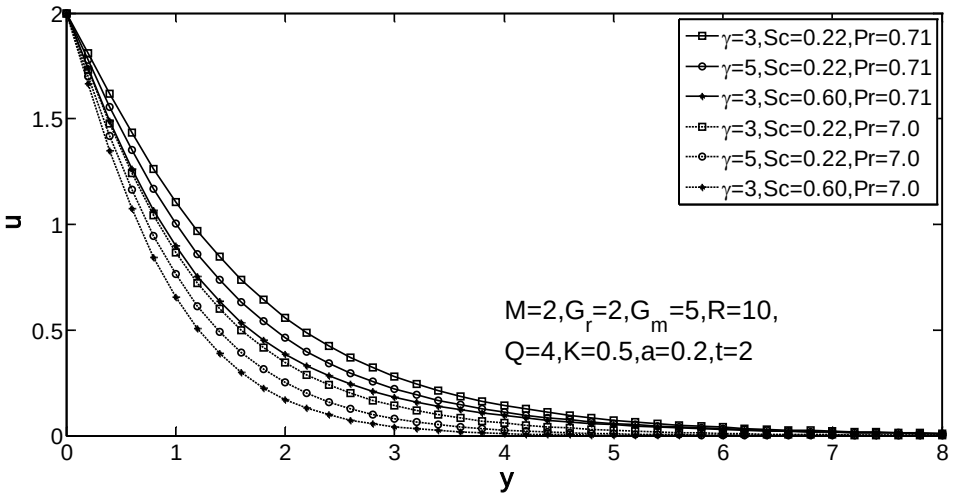

Figure-12: Velocity profiles for different values of γ, Sc and Pr

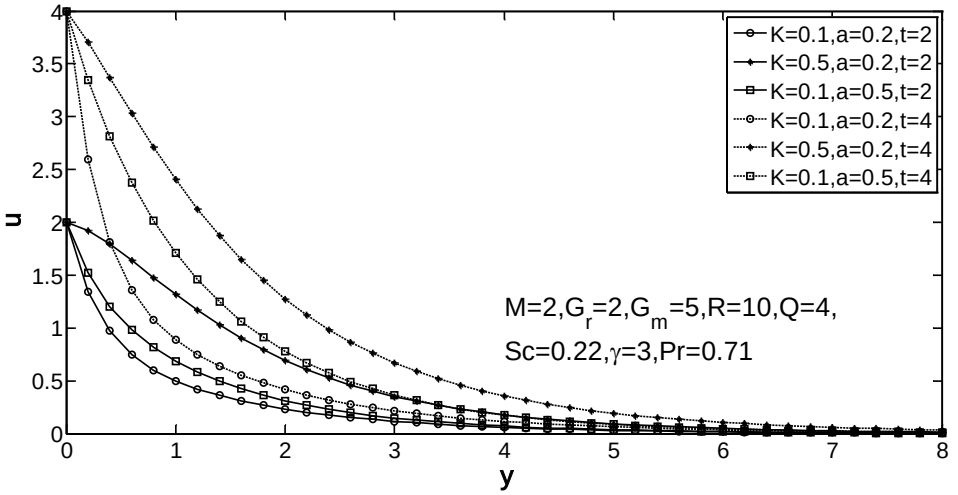

Figure-13: Velocity profiles for different values of K, a and t

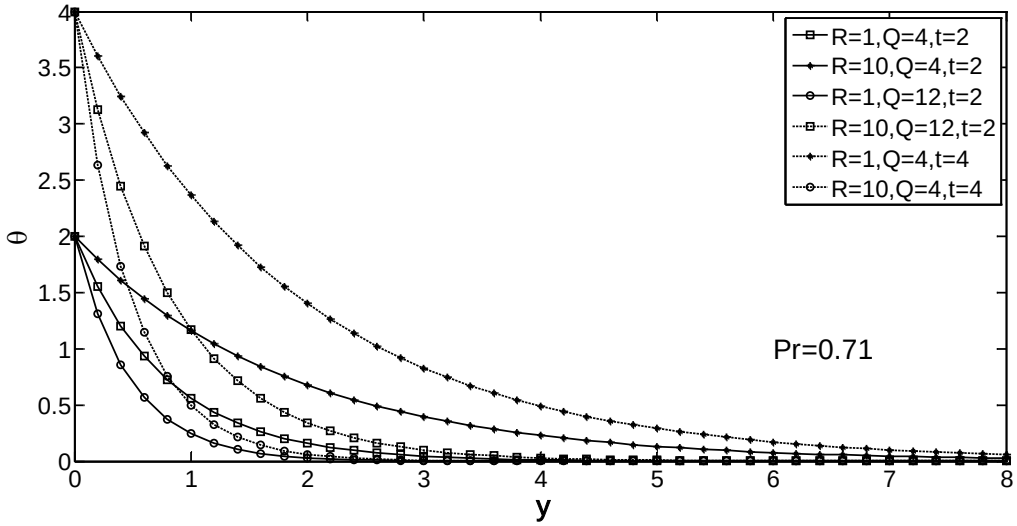

Figure-14: Temperature profiles for different values of R, Q and t

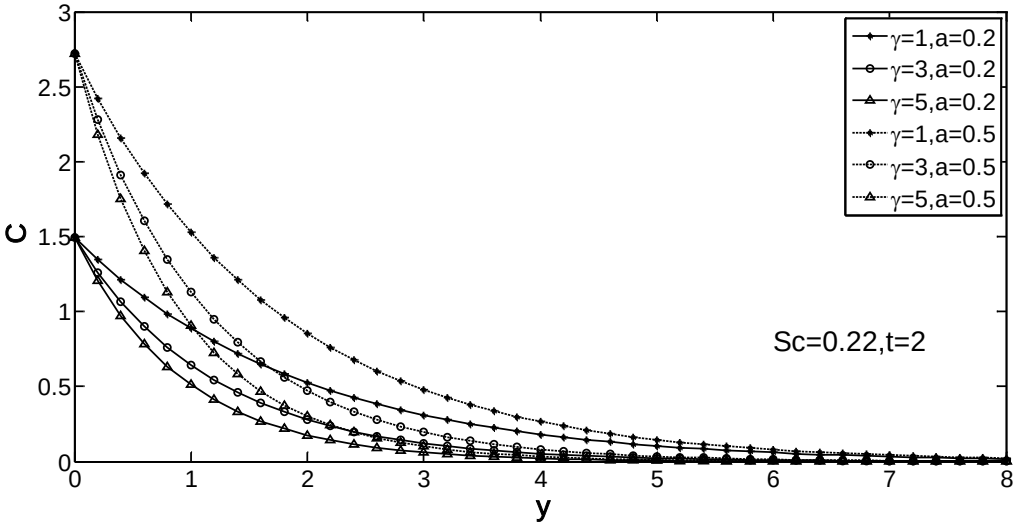

Figure-15: Concentration profiles for different values of γ and a

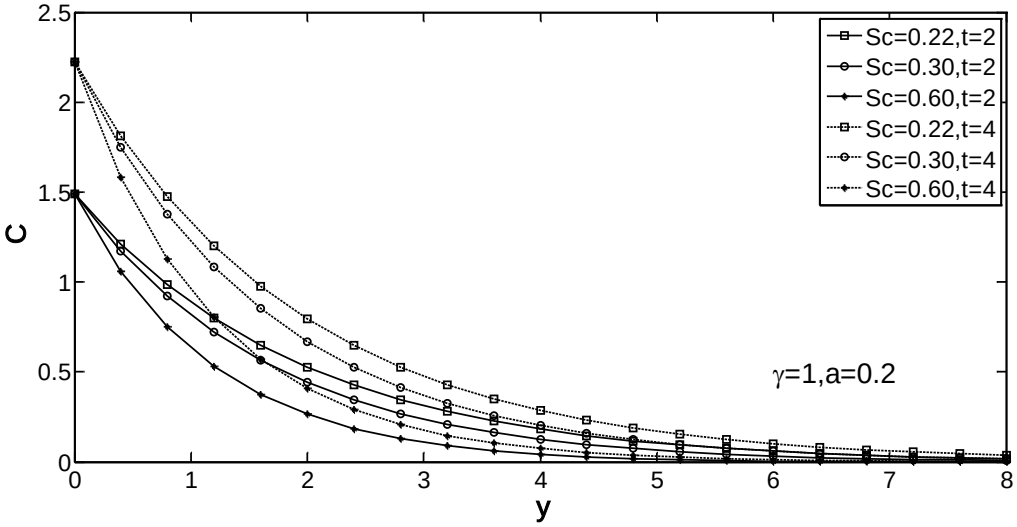

Figure-16: Concentration profiles for different values of Sc and t

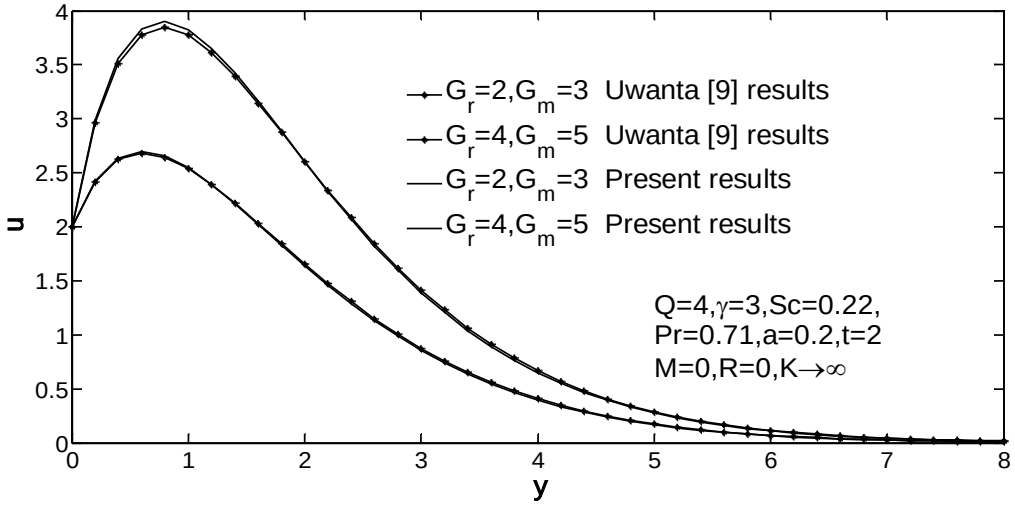

Figure-17: Comparison of velocity profiles for different values of G_r and G_m

Table-1: Numerical values of the skin friction coefficient (τ)

M	G_r	G_m	R	Q	K	Sc	γ	t	a	Pr	**Case(i)**	**Case(ii)**
2	2	5	1	4	0.1	0.22	3	2	0.2	0.71	4.1777	4.5184
3	2	5	1	4	0.1	0.22	3	2	0.2	0.71	4.5418	4.8729
2	**5**	5	1	4	0.1	0.22	3	2	0.2	0.71	3.2283	3.2702
2	2	**7**	1	4	0.1	0.22	3	2	0.2	0.71	3.2730	3.8295
2	2	5	**10**	4	0.1	0.22	3	2	0.2	0.71	4.0673	4.3698
2	2	5	1	**12**	0.1	0.22	3	2	0.2	0.71	4.2754	4.6419
2	2	5	1	4	**0.5**	0.22	3	2	0.2	0.71	0.0258	0.4922
2	2	5	1	4	0.1	**0.60**	3	2	0.2	0.71	4.4384	4.7111
2	2	5	1	4	0.1	0.22	**5**	2	0.2	0.71	4.2849	4.6055
2	2	5	1	4	0.1	0.22	3	**4**	0.2	0.71	8.4563	9.7407
2	2	5	1	4	0.1	0.22	3	2	**0.5**	0.71	3.6779	3.1604
2	2	5	1	4	0.1	0.22	3	2	0.2	**7.0**	4.4035	4.8189

Table-2: Numerical values of Nusselt number (Nu)

R	Q	Pr	t	**Case(i)**	**Case(ii)**
5	4	0.71	2	1.0517	1.4620
10	4	0.71	2	0.7767	1.0797
5	**12**	0.71	2	1.7925	2.4329
5	4	**7.0**	2	3.3023	4.5905
5	4	0.71	**4**	1.5690	2.8380

Table-3: Numerical values of Sherwood number (Sh)

Sc	γ	t	**Case(i)**	**Case(ii)**
0.22	3	2	1.7602	1.2517
0.60	3	2	2.9069	2.0672
0.22	**5**	2	2.2025	1.5956
0.22	3	**4**	3.3850	1.8673

5. CONCLUSIONS

In the case of cooling of the plate, the main findings of the present study corresponding to both the cases are:

- The velocity decreases with an increase in the magnetic parameter.
- An increase in Grashof number for heat and mass transfer or permeability parameter leads to an increase in the velocity.
- The velocity and temperature decreases with an increase in Prandtl number.
- The temperature increases with increasing radiation parameter whereas it sdecreases with increasing heat source parameter.
- As the Schmidt number or chemical reaction parameter increases, the concentration decreases.

REFERENCES

[1] Asogwa, K. K., Uwanta, I. J. and Aliero, A. A., Flow past an Exponentially Accelerated Infinite Vertical Plate and Temperature with Variable Mass Diffusion, International Journal of Computer Applications, Vol. 45, No.2, 2012.

[2] Chamkha, A. J., MHD Flow of a Uniformly Stretched Vertical Permeable Surface in the Presence of Heat Generation/ Absorption and a Chemical Reaction, Int. Comm. Heat Mass Transfer, Vol. 30, No.3, pp. 413-422, 2003.

[3] Hiremath, P. S. and Patil, P. M., Free Convection Effects on the Oscillatory Flow of a Couple Stress Fluid through a Porous Medium, Acta Mechanica, Vol. 98, No. 1, pp. 143-158, 1993.

[4] Muthucumaraswamy, R. and Vijayalakshmi, A., Hydromagnetic Flow past an Impulsively Started Infinite Vertical Plate with Variable Temperature and Mass Diffusion, Journal of Engineering Physics and Thermophysics, Vol. 78, No. 2, pp. 345-349, 2005.

[5] Pattnaik, P. K. and Biswal, T., Analytical Solution of MHD Free Convective Flow through Porous Media with Time Dependent Temperature and Concentration, Walailak Journal of Science and Technology, Vol.12, No.9, 2015.

[6] Rajesh, V. and Varma, S. V. K., Radiation Effects on MHD Flow through a Porous Medium with Variable Temperature or Variable Mass Diffusion, Journal of Applied Mathematics and Mechanics, Vol. 6, No. 1, pp. 39-57, 2010.

[7] Rajput, U. S. and Kumar, S., Radiation Effects on MHD Flow past an Impulsively Started Vertical Plate with Variable Heat and Mass transfer, Int. J. of Appl. Math. and Mech., Vol. 8 No. 1, pp. 66-85, 2012.

[8] Soundalgekar, V.M., Patil, M.R. and Jahagirdar, M.D., MHD Stokes problem for a vertical plate with variable temperature, Nuclear Engineering and Design, Vol. 64,
No. 1, pp. 39-42, 1981.

[9] Uwanta, I. J. and Sarki, M. N., Heat and Mass Transfer with Variable Temperature and Exponential Mass Diffusion, International Journal of Computational Engineering Research, Vol. 2, No. 5, 1487-1494, 2012.

NOMENCLATURE

B_0	External magnetic field
C	Dimensionless concentration
C_P	Specific heat at constant pressure
C^*	Species concentration
C_w^*	Concentration near the plate
C_∞^*	Concentration far away from the plate
D	Chemical molecular diffusivity
G_m	Mass Grashof number
G_r	Thermal Grashof number
g	Acceleration due to gravity
K	Dimensionless permeability parameter
K^*	Permeability of the porous medium
K_r^*	Chemical reaction parameter
M	Magnetic field parameter
Nu	Nusselt number
Pr	Prandtl number
Q	Heat source parameter
Q_0	Dimensional heat absorption coefficient
q_r^*	Radiative heat flux in the y^* - direction
R	Radiative parameter
Sc	Schmidt number
Sh	Sherwood number
T^*	Temperature
T_w^*	Temperature at the plate
T_∞^*	Temperature of the fluid far away from the plate
t	Dimensionless time
t^*	Time
u	Dimensionless velocity
u^*	Velocity of the fluid in the x^* - direction
u_0	Velocity of the plate
y	Dimensionless co-ordinate axis normal to the plate
y^*	Co-ordinate axis normal to the plate
β	Volumetric coefficient of thermal expansion
β^*	Volumetric coefficient of concentration expansion
γ	Dimensionless chemical reaction parameter
κ	Thermal conductivity of the fluid
μ	Coefficient of viscosity
ν	Kinematic viscosity
ρ	Density of the fluid
σ	Electric conductivity
τ	Shearing stress
θ	Dimensionless fluid temperature

Subscripts

w	Conditions on the wall
∞	Free stream conditions

Source of support: Nil, Conflict of interest: None Declared.

